Mechanisms of Exchange Interactions in Some Transition Metal Carboxylates, Sulfates, and Chlorides

Yurii V. Rakitin and Vladimir T. Kalinnikov

N. S. Kurnakov Institute of General and Inorganic Chemistry
of the Academy of Sciences of the USSR, Moscow, USSR

Mikhail V. Eremin

Kazan State University, Kazan, USSR

Experimental data on magnetic properties of dimeric carboxylates, $[LM(OOCR)_2]_2$, and polymeric sulfates $(N_2H_5)_2M(SO_4)_2$ and chlorides $AMCl_3$, where M is a transition metal, are analyzed using the exchange channel model described elsewhere. The model is shown to readily explain considerable variations of exchange parameters in the carboxylate series (M = Ti(III), V(III), Mn(II), Ni(II), and Cu(II)). Analysis of exchange parameter values reveals that only little exchange occurs across the M–O–S–O–M π-system in metal sulfates. Evidence is presented of direct exchange in the chlorides, $AMCl_3$.

Key words: Exchange interactions in isostructural series

1. Introduction

Despite considerable progress in exchange parameter calculations, the Goodenough-Kanamori semiempirical rules [1] retain their value as the simplest and often quite reliable means of predicting the sign and even the magnitude of exchange interactions.

The exchange channel model described in [2, 3] and theoretically analyzed in [4] reveals simple relationships between exchange parameter values in isostructural series and can therefore be considered as a useful supplement to the above mentioned rules.

In this work we apply the exchange channel model to the determination of exchange mechanisms operating in some transition metal dimeric carboxylates and polymeric sulfates and chlorides.

Prior to analysis of experimental data, the theory developed in [4] will briefly be summarized.

2. Theory

Consider a dimeric unit (isolated or incorporated into a more complex system) comprising mononuclear fragments a and b which are in orbitally nondegenerate states. Molecular spin-orbitals of these fragments (MO) will be denoted $|\gamma_a q_a \sigma_a\rangle$ and $|\gamma_b q_b \sigma_b\rangle$. Here γ is the irreducible representation of the local point group symmetry to which a given orbital belongs, q is a representation row, and σ is an electron spin projection.

The corresponding effective exchange Hamiltonian has the form [4]

$$\hat{H}_{ex} = \sum_{\gamma_a \gamma_b} \left[\frac{1}{4} + \frac{\hat{S}_{\gamma_a}\hat{S}_{\gamma_b}}{4S_{\gamma_a}S_{\gamma_b}} \right] J_{\gamma_a \gamma_b} \tag{1}$$

where the summation is over half-filled orbitals.

Each of the $J_{\gamma_a \gamma_b}$ parameters represents a sum of ferromagnetic and anti-ferromagnetic contributions.

Antiferromagnetic contributions arise from one-electron interactions and can be written in the form

$$
\begin{aligned}
J_{\gamma_a \gamma_b}^{(1)} = -2 \sum_{q_a q_b} \big[&\langle \gamma_a q_a | \hat{h}_a + \hat{h}_b | \gamma_b q_b \rangle \langle \gamma_b q_b | \gamma_a q_a \rangle \\
&- \sum_{q_a'} \langle \gamma_a q_a | \hat{h}_a | \gamma_a q_a' \rangle \langle \gamma_a q_a' | \gamma_b q_b \rangle \langle \gamma_b q_b | \gamma_a q_a \rangle \\
&- \sum_{q_b'} \langle \gamma_b q_b | \hat{h}_b | \gamma_b q_b' \rangle \langle \gamma_b q_b' | \gamma_a q_a \rangle \langle \gamma_a q_a | \gamma_b q_b \rangle \\
&+ \sum_{\gamma_a' q_a'} \frac{n_{\gamma_a'}}{[\gamma_a']} \langle \gamma_a q_a | \hat{h}_a | \gamma_a' q_a' \rangle \langle \gamma_a' q_a' | \gamma_b q_b \rangle \langle \gamma_b q_b | \gamma_a q_a \rangle \\
&+ \sum_{\gamma_b' q_b'} \frac{n_{\gamma_b'}}{[\gamma_b']} \langle \gamma_b q_b | \hat{h}_b | \gamma_b' q_b' \rangle \langle \gamma_b' q_b' | \gamma_a q_a \rangle \langle \gamma_a q_a | \gamma_b q_b \rangle \big]
\end{aligned}
\tag{2}
$$

This result was obtained on the assumption of collinearity of like axes in local coordinate systems attached to mononuclear fragments, and realness of overlap and exchange integrals, $\langle \gamma_a q_a | \gamma_b q_b \rangle$ and $\langle \gamma_a q_a | \hat{h} | \gamma_b q_b \rangle$, respectively.

The sums in (2) run over all half-filled orbitals q_a (q_b) belonging to irreducible representations γ_a (γ_b). Symbol n_γ stands for the number of electrons in a subshell with the γ symmetry, $[\gamma]$ is the representation dimension. The $\sum_{\gamma_a' q_a'}$ sums are understood to run over all orbitals not identical to γ_a.

Interelectronic repulsion described by operators $\hat{g}_{ij}$ leads to exchange coupling in which ferromagnetic terms prevail

$$
\begin{aligned}
J_{\gamma_a \gamma_b}^{(2)} = -2 \sum_{q_a q_b} \big[&\langle \gamma_{a_1} q_{a_1} \gamma_{b_2} q_{b_2} | \hat{g}_{12} | \gamma_{a_2} q_{a_2} \gamma_{b_1} q_{b_1} \rangle \\
&- \sum_{q_a' q_b'} \langle \gamma_{a_1} q_{a_1} \gamma_{b_2} q_{b_2} | \hat{g}_{12} | \gamma_{a_1} q_{a_1}' \gamma_{b_2} q_{b_2}' \rangle \langle \gamma_a q_a' | \gamma_b q_b \rangle \langle \gamma_b q_b' | \gamma_a q_a \rangle \big]
\end{aligned}
\tag{3}
$$

As intrafragment interactions are much stronger than interfragment ones, we have [3]

$$\hat{S}_{\gamma_a}/S_{\gamma_a} = \hat{S}_a/S_a, \ \hat{S}_{\gamma_b}/S_{\gamma_b} = \hat{S}_b/S_b \tag{4}$$

which allows to re-write (1) in the form

$$\hat{H}_{ex} = \left[\frac{1}{4} + \frac{\hat{S}_a\hat{S}_b}{4S_aS_b}\right]\left(\sum_{\gamma_a\gamma_b} J_{\gamma_a\gamma_b}\right) \tag{5}$$

Lastly, omitting the constant we obtain the exchange Hamiltonian in a conventional form $(J\hat{S}_a\hat{S}_b)$

$$\hat{H}_{ex} = \left(\frac{\sum\limits_{\gamma_a\gamma_b} J_{\gamma_a\gamma_b}}{4S_aS_b}\right)\hat{S}_a\hat{S}_b \tag{6}$$

which gives for the effective Heisenberg-Dirac-Van-Vleck exchange parameter

$$J = \sum_{\gamma_a\gamma_b} J_{\gamma_a\gamma_b}/4S_aS_b \tag{7}$$

It follows from (2) and (3) that, when γ_a or γ_b are not one-dimensional representations, and MOs belonging to these are degenerate, $J_{\gamma_a\gamma_b}$ are sums of contributions from all possible types of interaction of MOs $|\gamma_a q_a\rangle$ and $|\gamma_b q_b\rangle$:

$$J_{\gamma_a\gamma_b} = \sum_{q_a q_b} J_{q_a q_b} \tag{8}$$

and

$$J = \sum_{ij} J_{ij}/4S_aS_b \tag{9}$$

where i and j run over unpaired electrons on a and b, respectively.

For example, let us consider a pair of exchange coupled ions having spins $S_a = S_b = \frac{3}{2}$ and local point group symmetries D_{4h} (see Fig. 1). According to (7)

$$J_{ab} = (J_{E_g^a E_g^b} + J_{B_{2g}^a B_{2g}^b} + J_{B_{2g}^a E_g^b} + J_{E_g^a B_{2g}^b})/g$$
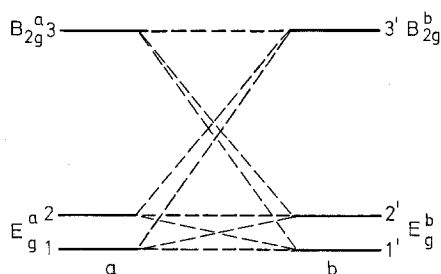

Fig. 1. Energy levels and possible pair exchange pathways for ions with $S_a = S_b = 3/2$ in tetragonal crystal fields

According to (2) and (3), exchange contributions from channels comprising half-filled degenerate orbitals can be further decomposed:

$$J_{E_g^a E_g^b} = J_{11'} + J_{12'} + J_{21'} + J_{22'};$$
$$J_{B_{2g}^a E_g^b} = J_{1'3} + J_{32'}; \quad J_{E_g^a B_{2g}^b} = J_{13'} + J_{23'}.$$

According to the Goodenough-Kanamori rules, a given exchange channel is antiferromagnetic if the corresponding overlap integral is of appreciable magnitude and ferromagnetic if $\langle \gamma_a q_a | \gamma_b q_b \rangle$ is zero. It should be noted that antiferromagnetic interactions are as a rule much stronger than ferromagnetic ones.

It has also been shown [4] that relatively weak dependence of individual exchange channel contributions on the number of electrons not involved in a given exchange channel is to be expected for a large class of systems where $\langle \gamma_a q_a | \gamma_b q_b \rangle \neq 0$ if $\gamma_a = \gamma_b$ and $q_a = q_b$. This assumption was tested against numerous experimental data to show that like channels give approximately the same contributions in isostructural compounds containing transition metal ions in the same or nearly the same oxidation states.

The theory described above can be summarized in the form of the following rule.

In systems with isotropic exchange in which $\langle \gamma_a q_a | \gamma_b q_b \rangle = \delta_{\gamma_a \gamma_b} \cdot \delta_{q_a q_b}$ the exchange parameter J represents the sum of exchange contributions from all interion one-electron channels divided by the number of such channels which is equal to $4 S_1 S_2$. These contributions depend only slightly on the number of unpaired electrons on the ions involved.

We can re-write (9) in the form

$$J_\Sigma = \sum_{ij} J_{ij} = 4 S_a S_b \cdot J \tag{10}$$

which suggests a more convenient formulation: the algebraic sum of contributions from all interionic one-electron channels is equal to the exchange parameter value, J, multiplied by the number of such channels.

Below, this approach is applied to the analysis of experimental data.

It is noteworthy that expressions (2) and (3) were obtained without any assumptions on the nature of the chemical bonds. Our conclusions should therefore be valid for ionic as well as covalent compounds. Some ionic systems have been considered in [4]. Here we extend our analysis to systems containing covalent bonds.

3. Dimeric Metal Carboxylates

Magnetic susceptibility, EPR and IR spectra, and other characteristics of a large class of transition metal carboxylate complexes $LM(OOCR)_2$ have been reported in [2]. A detailed analysis of the data obtained has shown these complexes to have dimeric structures of the type of copper acetate monohydrate, $[(H_2O)Cu(COCCH_3)_2]_2$ (Fig. 2). Complexes of Cu^{2+}, Ni^{2+}, Mn^{2+}, V^{3+}, and
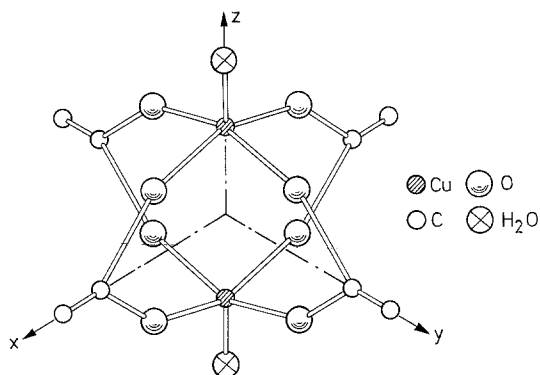
Fig. 2. Structure of copper acetate monohydrate, $[(H_2O)Cu(OOCCH_3)_2]_2$

Ti^{3+} exemplify isotropic exchange systems (the latter two metals give carboxylates with the cyclopentadienyl anion for L).

Symmetry considerations predict that of 25 types of $\langle d_{z^2}^a | d_{z^2}^b \rangle$ overlap integrals, only five ones that correspond to overlap of like orbitals ($\langle d_{z^2}^a | d_{z^2}^b \rangle$, $\langle d_{x^2-y^2}^a | d_{x^2-y^2}^b \rangle \cdots$ etc.) are nonzero. Hence, exchange contributions in metal carboxylates should exhibit low sensitivity to change of the metal.

According to [2], the largest exchange contributions arise from orbitals with the largest overlaps. It is clear from Fig. 2 that two exchange mechanisms can operate in the compounds under discussion: direct exchange where the $d_{z^2}^a - d_{z^2}^b$ channel is the most important one, and delocalization exchange across the M–O–C–O–M bond system. The importance of the latter mechanism depends to a considerable extent on overlap between M and O orbitals in the mononuclear fragment LMO_4.

Group theory analysis of tetragonal-pyramidal complexes reveals that the metal $d_{x^2-y^2}$ (σ-bond) and d_{xy} (π-bond) orbitals have the largest overlaps with oxygen

Table 1. Half-filled orbitals and sums of contributions to exchange parameters for systems $[LM(OOCR)_2]_2$ (I) and $(N_2H_5)M(SO_4)_2$ (II), in which pair exchange is described by the Hamiltonian $-2J\hat{S}_1\hat{S}_2$

	M	Half-filled orbitals	J (cm^{-1})	$4S_1S_2J$ (cm^{-1})
	Ti^{3+}	d_{xy}	-500 ± 100	-500 ± 100
	V^{3+}	d_{xy}, d_{z^2}	-140 ± 20	-560 ± 50
I	Mn^{2+}	$d_{x^2-y^2}, d_{xy}, d_{z^2}, d_{xz}, d_{yz}$	-15 ± 2	-375 ± 50
	Ni^{2+}	$d_{x^2-y^2}, d_{xy}$	-140 ± 10	-560 ± 40
	Cu^{2+}	$d_{x^2-y^2}$	-170 ± 30	-170 ± 30
	Cu^{2+}	d_{z^2}	-1.3	-1.3
II	Ni^{2+}	$d_{z^2}, d_{x^2-y^2}$	-2.3	-9.2
	Mn^{2+}	$d_{z^2}, d_{x^2-y^2}, d_{xy}, d_{xz}, d_{yz}$	-0.38	-9.5

orbitals (see e.g. Ref. [5]). Thus, the most effective channels of superexchange are $d^a_{x^2-y^2}-\sigma_O-\sigma_C-\sigma_O-d^b_{x^2-y^2}$ and $d^a_{xy}-\pi_O-\pi_C-\pi_O-d^b_{xy}$ (see Fig. 3).

The top part of Table 1 contains information about dimeric transition metal acetates where exchange interactions are described by the spin Hamiltonian $\hat{H}=-2J\hat{S}_1\hat{S}_2$ (the J values, the $J_\Sigma=4S_1S_2J$ values, and the types of half-filled orbitals involved).

The data on copper and titanium complexes both of which contain one unpaired electron on the metal directly give contributions from the $d^a_{x^2-y^2}-d^b_{x^2-y^2}$ and $d^a_{xy}-d^b_{xy}$ channels. Though the M–O σ-overlap exceeds the π-one, contribution from the latter channel is greater by a factor of 3. This may be due to the fact that the unpaired electron from the d_{xy} orbital is involved in the conjugated O–C–O bond system characterized by strong delocalization (Fig. 3) which is not the case with the electron from the $d_{x^2-y^2}$ orbital.
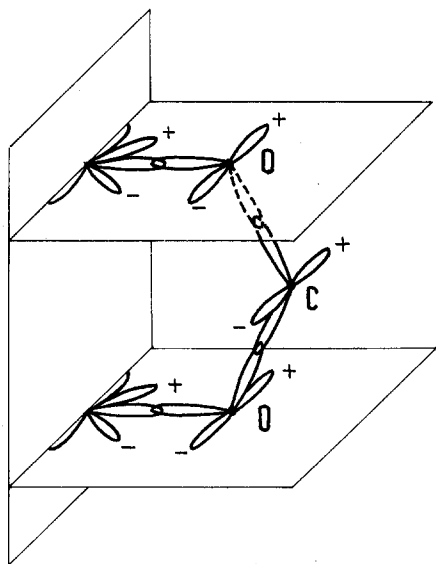

Fig. 3. σ- and π-bonds in the M–O–C–O–M fragment in dimeric carboxylates

The sum of exchange contributions remains practically the same on going from titanium to vanadium which implies that direct exchange ($d^a_{z^2}-d^b_{z^2}$) makes only a very small contribution (we neglect insignificant ferromagnetic (or anti-ferromagnetic, as it may prove to be the case in distorted structures) cross-contributions $J_{d_{xy}d_{z^2}}$ and $J_{d_{z^2}d_{xy}}$). In fact, setting these direct term and cross-terms equal to zero, we obtain

$$J_\Sigma = J_{d_{xy}d_{xy}} + J_{d_{z^2}d_{z^2}} + J_{d_{z^2}d_{xy}} + J_{d_{xy}d_{z^2}}$$
$$\approx -500 + 0 + 0 + 0 = -500 \; (\text{cm}^{-1})$$

which is in good agreement with the experimental value. With the metal-metal distance of about 3.7 Å [6], the absence of direct exchange is easy to comprehend.

Neglect of cross-contributions gives for the Ni complex

$$J_\Sigma = J_{d_{x^2-y^2}d_{x^2-y^2}} + J_{d_{x^2-y^2}d_{xy}} + J_{d_{xy}d_{x^2-y^2}} + J_{d_{xy}d_{xy}}$$
$$= (-170 \pm 30)\ \text{cm}^{-1} + 0 + 0 + (-500 \pm 100)\ \text{cm}^{-1} = (-670 \pm 120)\ \text{cm}^{-1}$$

which agrees satisfactorily with the experimental value for $4S_1S_2J$ ((560 $\pm 40)\ \text{cm}^{-1}$). This result lends support to the assignment of half-filled orbitals in Ni complexes based on crystal field theory calculations.

Three more exchange channels are added on going to the Mn complex. The observed $|J_\Sigma|$ value is, however, far beyond that one ($|-670 \pm 120|\ \text{cm}^{-1}$) which would account for super-exchange only ($J_{d_{xy}d_{xy}}$ and $J_{d_{x^2-y^2}d_{x^2-y^2}}$). This lowering of $|J_\Sigma|$ may be due to the neglect of twenty cross-channels among which ferromagnetic ones may prevail. However, contributions from cross-channels can hardly be large. It thus appears that in the Mn complex, the $d_{z^2}^a - d_{z^2}^b$ channel is also of little importance and direct Mn–Mn exchange does not occur.

Dimeric chromium (d^4, $S=2$) acetate differs strongly from the other acetato complexes. Formally, the value of $-500\ \text{cm}^{-1}$ for J in chromium acetate (see Ref. [7]) suggests that its magnetic properties can be explained by superexchange over the π-bond system (cf. Ti^{3+}). The exchange channel model, however, predicts for Cr^{2+}

$$J_\Sigma = 4S_1S_2J_{12} \approx -8000\ \text{cm}^{-1}$$

which makes it clear that the contributions from superexchange are negligibly small and implies a strong (of about $8000\ \text{cm}^{-1}$) direct exchange coupling across the $d_{z^2}^1 - d_{z^2}^2$ channel. This predicts a value of about $15000\ \text{cm}^{-1} \approx 40$ kcal/mol for the singlet-triplet splitting in the $d_{z^2}^a - d_{z^2}^b$ system which is indicative of the formation of the metal-metal bond. Our conclusion is in agreement with the structural data. The recent X-ray study of this compound [8] gave the Cr–Cr distance of 2.36 Å, well below the sum of the covalent radii.

4. Linear Chains $(N_2H_5)\ M^{2+}(SO_4)_2$

The structure of linear chains $(N_2H_5)M(SO_4)_2$ is depicted in Fig. 4. Their magnetic properties are described in [10]. It has been shown that interchain interactions via hydrogen bonds are exceedingly weak in such systems. The analysis of magnetic susceptibility data in terms of different exchange models has shown that isotropic exchange occurs in the $\text{Cu}^{2+}(d^9)$, $\text{Ni}^{2+}(d^8)$, and $\text{Mn}^{2+}(d^5)$ complexes. The exchange parameters corresponding to the exchange Hamiltonian $\hat{H} = -2J\sum_i \hat{S}_i \hat{S}_{i+1}$ are listed in the bottom part of Table 1 where types of orbitals constituting exchange channels are also indicated. We should note that the ordering of one-electron orbitals on the energy scale adopted in this work is derived from qualitative considerations. We however believe it to be rather realistic. In fact, metal ions are nearly octahedrally coordinated with four oxygen and two nitrogen atoms in the sulfates (Fig. 4). As oxygen gives rise to weaker CFs than nitrogen, such coordination results in a tetragonal crystal field with a strong axial component. In this case, two level schemes are possible: $d_{xy}, d_{x^2-y^2}, \{d_{xz}, d_{yz}\}, d_{z^2}$ and $d_{xy}, \{d_{xz}, d_{yz}\}$,

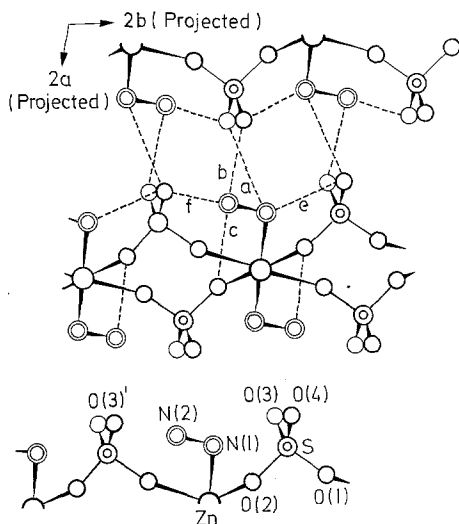**Fig. 4.** Structure of $(N_2H_5)_2Zn(SO_4)_2$. Hydrogen bonds are shown by dotted lines [9]

$d_{x^2-y^2}$, d_{z^2}. The former places one of the Ni unpaired electrons on the $\{d_{xz}, d_{yz}\}$ degenerate level which would be incompatible with isotropic exchange. This is why we have adopted the second variant.

Qualitative considerations also show that direct exchange can hardly occur in the compounds under discussion because of very large (of about 5.3 Å) metal-metal distances. Of superexchange channels, the σ-bond system M–O–S–O–M involving metal $d_{x^2-y^2}$ orbitals is quite analogous to that characteristic of the acetato complexes. The most effective π-superexchange channel should be that constructed from group π-orbitals comprising metal d_{xz} (d_{yz}) orbitals and conjugated π-bond system of the OSO fragment. This channel has geometric characteristics similar to those of the corresponding M–O–C–O–M channel in metal carboxylates. Lastly, small overlap of d_{z^2} orbitals should be mentioned which is due to their participation in the group σ- and π-bonds.

In agreement with what can be expected from the above considerations, copper complexes exhibit weak antiferromagnetic exchange. On going to Ni, the sum of the exchange channel contributions increases rapidly because of the addition of the σ-channel (Table 1 and Fig. 3). The addition of the π-channel in the Mn compound, however, causes no significant change of J_Σ comparable to that observed in the carboxylate series. This implies that the O–S–O conjugated π-system is by far less effective than the O–C–O one. The latter conclusion is in agreement with the well-known fact that propensity for the formation of π-bonds decreases on going from the second row to the third row elements (thus, oxygen forms O_2 molecules with one σ- and one π-bonds, while sulfur prefers to form σ-bonded chains –S–S–S–).

5. Metal Chlorides AMCl₃

Metal chlorides $AMCl_3$ form chains of octahedra sharing faces (Fig. 5) with M–Cl–M angles of about 90°. According to the Goodenough-Kanamori rules, appreciable
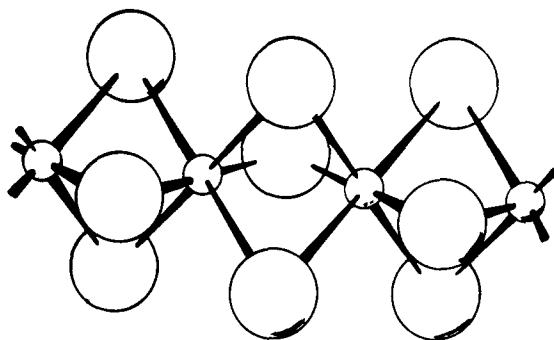
Fig. 5. Structure of chlorides $AMCl_3$. Outer-sphere single-charged cations A are not shown

superexchange can hardly be expected in these systems. The data in Table 2 confirm this suggestion. One can see that in systems in which only e_g orbitals are half-filled and where, consequently, maximum electron density axes coincide with the bond directions, the $|J_{\Sigma}|$ value is highly sensitive to variation of the M–Cl–M angle but remains below $50 \ \mathrm{cm}^{-1}$. It is clear that superexchange involving half-filled t_{2g} orbitals cannot give contributions exceeding markedly those from σ-channels because π-overlap of metal t_{2g} and ligand orbitals is smaller than σ-overlap of e_g orbitals. However, as indicated in Table 2, the $|J_{\Sigma}|$ value increases by a factor

Table 2. Magnetic parameters and structure characteristics of polymer chains $AMCl_3$ [11]

Compound	M–M (Å)	Half-filled orbitals	$J \ (\mathrm{cm}^{-1})$	$4S_1 S_2 J$ (cm^{-1})
$CsCuCl_3$	3.062	e_g^1	~ 0	~ 0
$CsNiCl_3$	2.97	e_g^1, e_g^2	-9	-36
$RbNiCl_3$	2.953	e_g^1, e_g^2	-11	-44
$(CH_3)_4NNiCl_3$	3.577	e_g^1, e_g^2	1.3	5.2
$RbVCl_3$	3.00	$t_{2g}^{\pm 1}, t_{2g}^0$	-105	-945
$CsCrCl_3$	3.11	$e_g^1, t_{2g}^{\pm 1}, t_{2g}^0$	-24	-384
$(CH_3)_4NMnCl_3$	3.25	$e_g^1, e_g^2, t_{2g}^{\pm 1}, t_{2g}^0$	-3.8	-95

exceeding 20 on going to $RbVCl_3$ ($^4A_{2g}$). A direct overlap of $t_{2g}^0 \equiv d_{z^2}$ orbitals (z is the three-fold axis) may be responsible for this effect. Direct exchange contributions are known to be highly sensitive to variation of metal-metal distances. Accordingly, the $|J_{\Sigma}|$ value decreases in the order $RbVCl_3$, $CsCrCl_3$, $(CH_3)_4NMnCl_3$ from 945 to $95 \ \mathrm{cm}^{-1}$, while the metal-metal distance only increases by 0.25 Å in the same series (from 3.00 to 3.25 Å). The value of $95 \ \mathrm{cm}^{-1}$ can be accounted for by superexchange. The conclusion that direct exchange occurs in the chlorides $AMCl_3$ agrees with the results reported in [12].

6. Conclusions

The available experimental data on magnetic properties of dimeric transition metal carboxylates, $[LM(OOCR)_2]_2$, and polymeric transition metal sulfates,

$(N_2H_5)_2M(SO_4)_2$, and chlorides, $AMCl_3$, are analyzed in terms of the exchange channel model. The model is shown to provide a ready explanation of considerable variations of exchange parameters in the series of carboxylates of Ti(III), V(III), Mn(II), Ni(II), and Cu(II). Metal-metal bonding is shown to occur in chromium acetate, but not in the manganese derivative. Analysis of exchange parameter values for the sulfates reveals that no π-bonding occurs in the O–S–O bridges. Evidence is presented of direct exchange in the chlorides, $AMCl_3$.

References

1. Anderson, P.: Solid State Phys. **14**, 79 (1963)
2. Kalinnikov, V. T.: Thesis, Institute of General and Inorganic Chemistry of the Academy of Sciences of the USSR, Moscow, 1975
3. Rakitin, Yu. V., Eremin, M. V., Kalinnikov, V. T.: Dokl. Akad. Nauk SSSR **233**, 71 (1977)
4. Eremin, M. V., Rakitin, Yu. V.: Phys. Status Solidi (in print)
5. Ballhausen, C. J., Gray, H. B.: Inorg. Chem. **1**, 111 (1962)
6. Aleksandrov, G. G., Struchkov, Yu. T. Zh. Strukt. Khim. **11**, 497 (1970)
7. Martin, R. L., in: New pathways in inorganic chemistry, Ebsworth, E. A. V., Mattock, A. G., and Sharpe, A. G., Eds. London: Cambridge University Press, 1968
8. Cotton, F. A., de Boer, B. G., La Parade, M. D., Pipal, J. K., Ucko, D. A.: J. Am. Chem. Soc. **92**, 2928 (1970)
9. Prout, C. K., Powell, H. M.: J. Chem. Soc. 4177 (1961)
10. Witteween, H. T., Reedijk, J.: J. Sol. State Chem. **10**, 151 (1974)
11. Ackerman, J. F., Cole, G. M., Holt, S. L.: Inorg. Chim. Acta **8**, 323 (1974)
12. Gray, I. E., Smith, P. W.: Australian J. Chem **24**, 73 (1971)